Key Engineering Materials Vols. 257-258 (2004) pp. 3-8
online at http://www.scientific.net

Chip Formation Behaviour in Ultra-Precision Cutting of Electroless Nickel Plated Mold Substrates

J. Yan, T. Sasaki, J. Tamaki, A. Kubo and T. Sugino

Department of Mechanical Engineering, Kitami Institute of Technology
Koen-Cho 165, Kitami, Hokkaido 090-8507, Japan

Keywords: Diamond Turning, Ultra-Precision Cutting, Electroless Nickel Plating, Mold Fabrication, Chip Formation, Cutting Fluid, Surface Integrity

Abstract. Electroless nickel plating is used in mold manufacturing industries as a surface processing technology for providing hard, ductile, wear resistant and corrosion-resistant surfaces. In this work, we conducted single point diamond turning experiments on electroless nickel plated substrates at machining scales from the nanometric to the micrometer level, and the machining behaviour was investigated through examining the chip morphology and surface texture. Emphatically, the effect of cutting fluid was investigated in detail. The results showed that the chip formation mechanisms in dry cuts and wet cuts are significantly different. Dry cuts cause splitting, adhesion, folding and secondary deformation of the chips, leading to surface defects. The results indicated that an effective supply of cutting fluid to the cutting region is essentially important to achieve high quality surfaces.

Introduction

The use of electroless nickel plating on industrial parts is continually increasing. Electroless nickel plating is primarily used to provide hard, ductile, wear resistant, and corrosion-resistant surfaces and to provide uniform build-up on complex shapes. Particularly, it is widely used in mold manufacturing industries as a surface processing technology for the mold substrates made of high hardness materials. In contrast to conventional electrolytic processes, electroless nickel plating does not use an electric current to produce a deposit, but operates chemically. Recent applications of electroless nickel plated molds include those for fabricating plastic optical parts such as aspheric and Fresnel lenses, mirrors and the light guiding plate of liquid crystal displays (LCD), and so on [1-2].

Most of these applications involve the ultra-precision cutting of fine grooves on the electroless nickel-plated mold substrates; the surface smoothness and form accuracy of the micro grooves need to be extremely high. In order to meet these demands, deliberately sharpened cutting tools made of single crystal diamond are required, and the machining scale usually ranges from the nanometer to the micrometer level, depending on the objectives. However, sometimes the machined surfaces are not produced as desired, but have defects such as burs, projections, ripples and so on. These defects seriously affect the quality and stability of the final product. For specific applications, post-polishing is required to finish the diamond machined parts and obtain a better surface integrity [3]. However, polishing is only capable of finishing components with large diameters, and not applicable to those components with extremely small apertures and micro-grooves. Thus, it is important to optimally control the ultra-precision machining process of electroless nickel to fabricate defect-free surfaces directly. However, up to date, there is little available literature on this issue, and the factors governing the formation of surface defects have not been clarified.

In the present work, we conducted ultra-precision cutting experiments on electroless plated nickel and some fundamental aspects of surface formation and chip generation were investigated. Especially when machining fine micro grooves and components with large curvatures, the lack of cutting fluid in the cutting region may be one of the possible reasons causing surface defects. Therefore, in this work, the effect of cutting fluid on the chip formation mechanism was emphatically examined.

Experimental Procedures

The experiments of this study were carried out on an ultraprecision diamond lathe, NACHI-ASP15. This machine has an air bearing spindle, two perpendicular slide tables (*X*-axis and *Z*-axis) and a rotary table (*B*-axis). The *X* and *Z* tables are supported by high-stiffness hydrostatic bearings and are driven by AC servomotors via hydrostatic screws, allowing smooth nanometric movement with negligible mechanical friction. Laser hologram scales are used to accurately position the *X* and *Z* tables. The *B*-axis table is supported by hydrostatic bearings and driven by a friction drive in order to prevent from non-driven movement. Under numerical control, the *X* and *Z* tables can be moved at 10 nm per step and the *B*-table can be rotated with an angular resolution of 0.001˚. To isolate the machine from environmental vibration, the main section of the system was fixed to a granite bed, which is supported by air mounts.

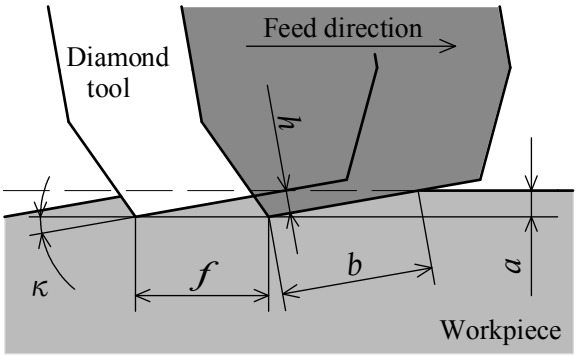

Fig. 1 Schematic of the machining model.

Electroless nickel plated steel substrates, 50 mm in diameter, 5 mm in thickness, were used in the experiments. A 200 μm thick layer of nickel has been deposit on the steel substrate by electroless plating. Heat treatment was performed after the plating at a temperature of 180 ˚C for two hours and then cooled down to the room temperature slowly. These conditions provide an complete amorphous microstructure with a Vickers hardness of 580. The workpiece was then bonded to a diamond-turned aluminium blank using a heat-softened glue and vacuum-chucked on the machine spindle.

A new single-crystal diamond tool having a 1.5 mm long straight cutting edge and a 135˚ included angle was used for cutting. The tool rake angle was 0˚, and the relief angle was 6˚. Figure 1 shows the schematic of the machining model.

Undeformed chip thickness *h* was varied from 0.02 to 5 μm by varying the tool feed *f* from 2 to 47 μm and the cutting edge angle κ in the range of 0.5 to 6˚. The depth of cut *a* was varied in the range of 2 ~ 5 μm. The spindle rotation rate was constant at 1000 rpm. Face turning was performed at the diameter range from 10 to 50 mm with a corresponding cutting speed of 94 ~ 470 m/min. Dry cuts and wet cuts were performed respectively for each condition. Kerosene mist, namely a mixture of high pressure (0.2MPa) air and kerosene liquid, was used as cutting fluids in the wet cuts. The jet of mist was precisely directed to the cutting region with two nozzles, one from the side and the other from the top of the rake face of the cutting tool.

The machined surfaces were observed using a scanning electron microscope (SEM) and measured using a laser-probe non-contact three dimensional profiling instrument, NH-3SP, and an atomic force microscope (AFM). Chips removed from the specimen were observed with the SEM.

Results and Discussion

Surface Texture and Surface Roughness. Electroless nickel is a ductile material; thus, theoretically the machined surface will be generated by the tool-workpiece transcription, yielding regular saw-toothed sectional profiles. Therefore, the maximum height of the surface profile, namely the peak-valley surface roughness R_y, can be predicted by

$$R_y = \frac{f}{\cot\kappa - \cot(\varepsilon + \kappa)}, \tag{1}$$

where *f* is the tool feed and ε is the included angle of the tool. In this study, first, the surface roughness was measured for various conditions and the experimental values were compared with the theoretical

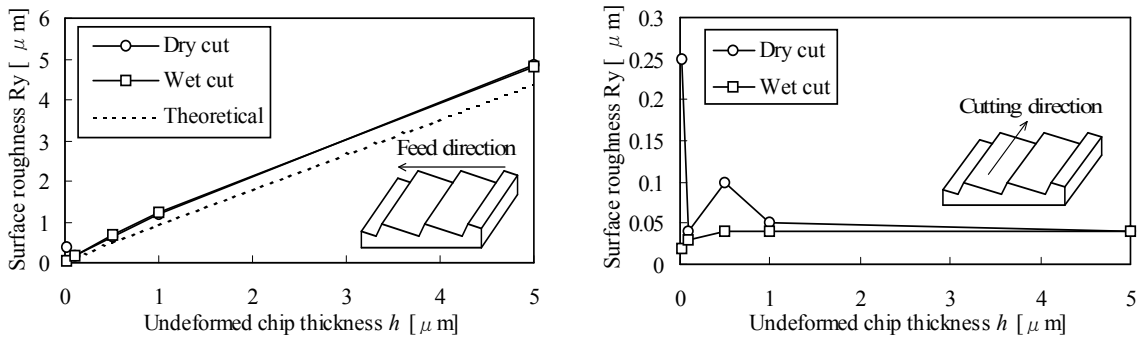

Fig. 2 Changes of surface roughness R_y with undeformed chip thicknesses. The surface roughness was measured along (a) the tool feed direction and (b) the cutting feed direction, respectively.

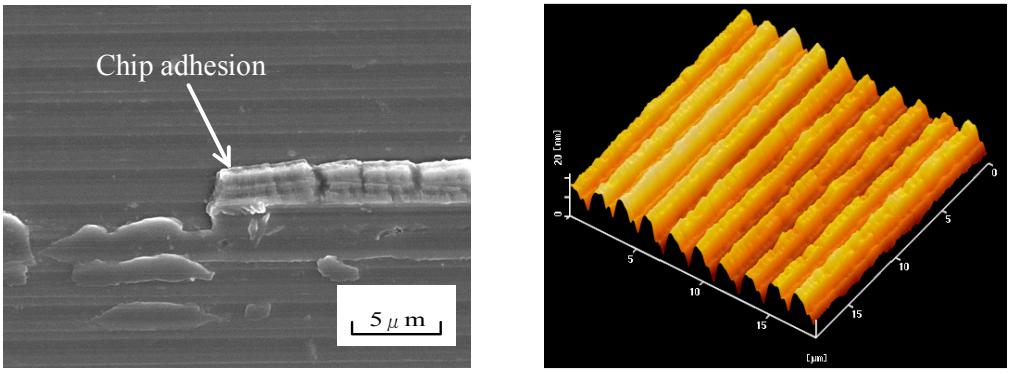

Fig. 3 Machined surfaces at an undeformed chip thickness of 0.02 μm. (a): SEM of the dry cut surface, (b): AFM of the wet cut surface.

values. For all the conditions, the surface profile measurements were done along two perpendicular directions, the cutting direction and the feed direction, respectively.

Figure 2 (a) and (b) show the results of surface roughness R_y at various undeformed chip thicknesses measured along the cutting direction and feed direction, respectively. Both the results of dry cuts and wet cuts are given. For the wet cuts, the change of surface roughness with undeformed chip thickness agrees well with the theoretical trend, indicating a precise tool-workpiece transcription. However, for the dry cuts, significant deviations of the measured value from the theoretical value can be seen at the undeformed chip thicknesses of 0.02 μm in Fig. 2 (a), and at 0.02 and 0.5μm in Fig.2 (b). Next, the surfaces cut at undeformed chip thicknesses of 0.02 and 0.5 μm were examined in detail.

Figure 3 (a) is an SEM photograph of the dry cut surface at undeformed chip thicknesses of 0.02 μm. Although a part of the surface is smooth with regular grooves, a few projections can be observed on the surface. It was these projections that led to the abnormally high surface roughness. One of the reasons of these projections would be the adhesion of the chips, as described later. However, no such projections were observed on the wet cut surface. Figure 3 (b) is an AFM image of the wet cut surface at the same undeformed chip thicknesses. The surface is extremely smooth without any projections. The surface consists of nanometric level regular grooves formed by the periodical tool feeds. The surface roughness is 0.015 μm R_y, which is similar to the theoretical value.

Figure 4 (a) and (b) show the profiles of the surfaces cut at an undeformed chip thickness of 0.5 μm under dry and wet conditions, respectively. These profiles were both measured along the cutting direction, that is, the longitudinal direction of the grooves. In Fig. 4 (a), periodical waviness approximately 0.1 μm in height, 50 μm in length can be observed. Although the height of this waviness

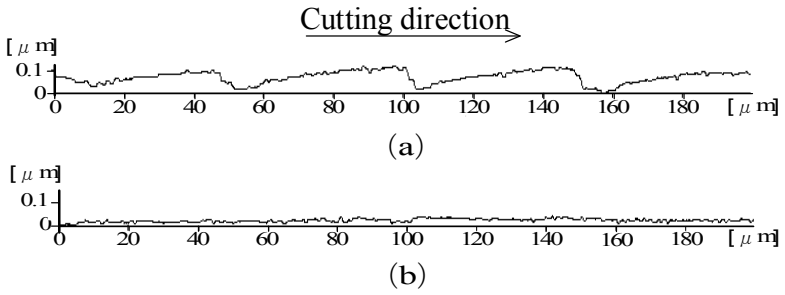

Fig. 4 Surface profiles measured along the cutting direction at an undeformed chip thickness of 0.5 μm. (a): dry cut, (b): wet cut.

is lower than that of the tool feed marks and is not obvious on the profile measured along the feed direction, they are akin to chatter marks and degrade the flatness of the micro grooves. This surface feature is thought to be attributed to the low amplitude vibration of the tool caused by chip folding, as described later. However, in wet cuts, as shown in Fig. 4 (b), the waviness could not be observed. Instead, the grove surface was extremely smooth, having nanometric surface roughness.

Chip Morphology. Figure 5 (a) and (b) show the SEM photographs of the chips generated at an undeformed chip thickness of 0.02 μm under dry and wet conditions, respectively. In Fig. 5 (a), the chips are in the form of narrow fibres whose widths are significantly smaller than the width of cut *b*. This indicates that the chip has been split into many sections along the cutting edge. In Fig. 5 (b), the chips are in the form of flow type ribbons, whose widths are the same as the width of cut *b*.

In dry cuts, high temperature is generated in the cutting region, which elevates the surface energy of both the newly generated chip and the workpiece. Therefore, these surfaces are physically and chemically active and easy to be adhered to each other. The adhesion will become significant when undeformed chip thickness is extremely small, where the effective rake angle caused by the edge radius becomes a high negative value. This situation makes the chip flow difficult and gives rise to built-up edges. Therefore, the actual cutting conditions will differ with positions along the cutting edge, thus the chips are split to narrow fibres. These small narrow chips are easy to be wrapped into the cutting region again and adhered to the workpiece surface by the squeezing of the tool, as in Fig. 3 (a). However, in wet cut, the cutting region is cooled, so that the surface energy of the chips and the workpiece are low and difficult to adhere. Due to the lubrication effect of the kerosene, the friction between the tool and the chip is also largely reduced, therefore the built-up edge is insignificant and the chip forms as ribbons and flows fluently along the tool rake face.

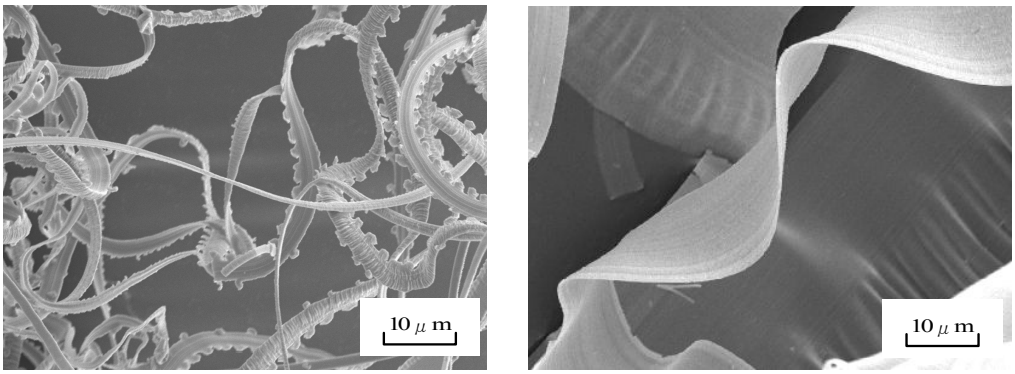

(a) (b)

Fig. 5 SEM photographs of the chips generated at an undeformed chip thickness of 0.02 μm. (a): dry cut, (b): wet cut.

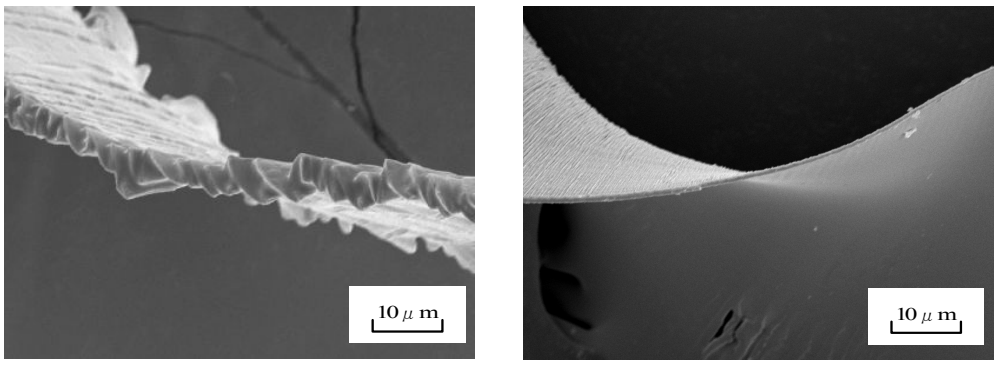

(a) (b)

Fig. 6 SEM photographs of the chips generated at an undeformed chip thickness of 0.1 μm. (a): dry cut, (b): wet cut.

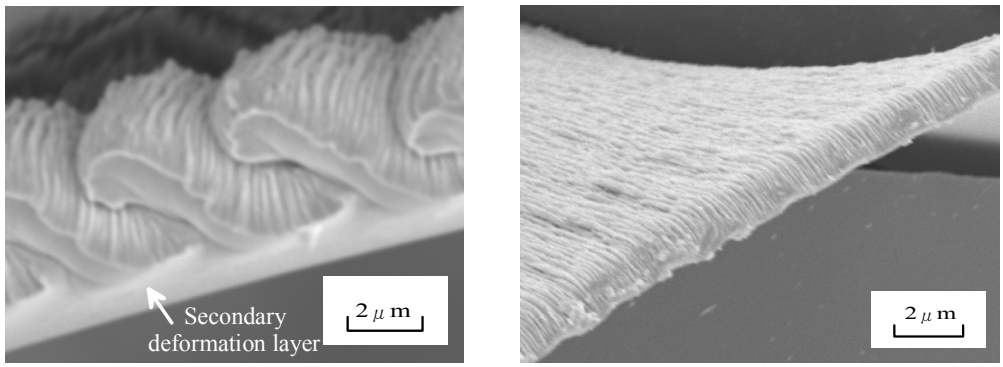

(a) (b)

Fig. 7 SEM photographs of the chips generated at an undeformed chip thickness of 0.5 μm. (a): dry cut, (b): wet cut.

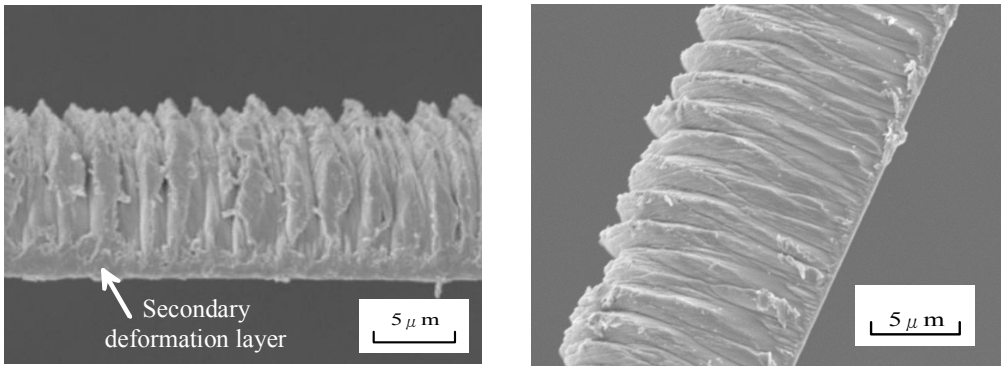

(a) (b)

Fig. 8 SEM photographs of the chips generated at an undeformed chip thickness of 5 μm. (a): dry cut, (b): wet cut.

Figure 6 (a) and (b) show the SEM photographs of the chips generated at an undeformed chip thickness of 0.1 μm under dry and wet conditions, respectively. In Fig. 6 (a), the chip is in the general form of a ribbon, but is not flat and folded at a space of several μms. As a contrast, in Fig. 6 (b), the chip is in the form of a flat and smooth ribbon, whose thickness is uniform. The folding of the chip in dry cut is due to the chip-tool friction, which prevent the chips from flowing along the rake face. Especially when the chip is very thin, it is easy to be bended and folded, as has been observed in the nanometric level dry cutting of electroplated copper [4]. The chip folding can further cause stick-slips between the tool and the chip, and simulate low amplitude vibration of the tool. As a result, low amplitude waviness (ripples) as shown in Fig.4 (a) is formed on the finished surface.

Figure 7 (a) and (b) show the SEM photographs of the chips generated at an undeformed chip thickness of 0.5 μm under dry and wet conditions, respectively. In Fig. 7 (a), the folding of the chip is also significant and the folding space is a few times larger than that in Fig. 6 (a). What to be note is that one side of the chip which contacts with the tool is smooth, beneath which is a secondary deformation layer, as indicated by an arrow. This deformation layer is thought to be generated by the severe shear force caused by the friction between the rake face and the newly generated chip surface. In Fig. 7 (b), the chip is straight and unfolded, with lamella structure. The secondary deformation layer is very thin.

Figure 8 (a) and (b) show the SEM photographs of the chips generated at an undeformed chip thickness of 5 μm under dry and wet conditions, respectively. The chips are very similar in shape. Both of them are typical shear type chips seen in conventional metal cutting. The only difference is that the chip in Fig. 8 (a) has a very thick deformation layer beneath the surface contacting with tool, whereas in Fig. 8 (b), the deformation layer is illegible. Similar phenomenon was also observed at undeformed chip thickness of 1 μm. These results indicate that in dry cut at a large undeformed chip thickness, the friction between the tool and the chip surface is by far severe than that in wet cut.

The intensive friction between the tool rake face and the chip also lead to severe tool wear. It is known that in the cutting of electroless nickel, the general wear pattern consists of grooves and crater wear on the rake face and slight chipping on the cutting edge [5]. Compared to the cutting of other metal materials such as aluminium and copper, electroless nickel cutting causes significantly deep and long wear grooves and craters on the tool rake face. This distinguishing feature indicates that the contact length between the tool and the chip is very long and the contact pressure maybe very high. It is these intensive contact conditions that give rises to the chip folding at a small undeformed chip thickness, and the secondary deformation layer in the chip at a large undeformed chip thickness.

Summary

The effects of cutting fluid on diamond turning of electroless plated nickel were investigated. The results showed that chip formation mechanisms of dry cuts and wet cuts are significantly different. In dry cuts at an extremely small undeformed chip thickness (0.02 μm), chip splitting and chip adhesion occurs, forming surface projections. As undeformed chip thickness increases (0.5 μm), surface waviness is formed by the stick-slips resulting from chip folding. At an undeformed chip thickness larger than 1 μm, a thick secondary deformation layer is generated in the chip near the chip-tool contact boundary. However, in wet cuts, very smooth surfaces were produced with yielding flow and shear type ribbon chips. The results from this investigation indicate that the cutting fluid plays an important role in the ultra-precision cutting of electroless nickel. The lack of cutting fluid causes surface defects such as projections and ripples. It is essentially important to effectively supply the cutting fluid to the cutting region, especially when undeformed chip thickness is extremely small.

References

[1] S.C. Fawcett and D. Engelhaupt: Development of Wolter I X-ray Optics by Diamond Turning and Electrochemical Replication, Prec. Eng., Vol. 17 (1995), p. 290.

[2] K. Tanaka: Ultra-precision Machining Technology and that examples for LCD, J. Jap. Soc. Abra. Tech., Vol. 46 (2002), p. 163.

[3] R.E. Parks and C.J. Evans: Rapid Post-polishing of Diamond-turned Optics, Prec. Eng., Vol. 16 (1994), p. 223.

[4] N. Ikawa, S. Shimada, R.R. Donaldson, C.K. Syn, J.S. Talor, G. Ohmori, H. Tanaka and H. Yoshinaga: Chip Morphology and Minimum Thickness of Cut in Micromachining, J. Jap. Soc. Prec. Eng., Vol. 59 (1993), p. 673.

[5] E. Paul, C.J. Evans, A. Mangamelli, M.L. McGlauflin and R.S. Polvani: Chemical Aspects of Tool Wear in Single Point Diamond Turning, Prec. Eng., Vol. 18 (1996), p. 4.